# Frequency Excursion of Three Area H-T-H Deregulated System Optimized by BF Algorithm with Energy Storage Devices

**A. J. Raja**

A. Assistant Director, National Power Training Institute, Ministry of Power, Govt. of India, Sector-33, Near NHPC, Faridabad – 121003, Haryana,
E-mail: jrajaj1980@gmail.com, jraja@npti.in

**C. Christober Asir Rajan**

B. Assocaite Professor, Faculty of Electrical Engineering, Pondicherry Engineering College, Affiliated to Pondicherry University, Kalapet, Puducherry.

***Abstract :*** *This paper adresses the results of an analysis of the dynamic performance of tie line power and frequency control, for an Automatic Generation Control (AGC) in three-area power system after deregulation, based on Bacterial Foraging (BF) optimization technique with the presence of energy storage devices. A comparative transient performance of AGC Control with SMES and CES are analyzed in deregulated environment. A maiden attempt has been made by implementing AGC with SMES, CES in deregulated environment with BF based optimal tuning of three area interconnected power system. The proposed method optimizes the parameter of integral controller by selecting the optimal gain which drives the change in frequency in the two areas and tie line power flow to zero within the shortest time span. The conventional three areas AGC system is modified to take into account the effect of bilateral contracts on the dynamics. In the considered power system, each area contains three GENCOs, three DISCOs and three area includes H-T-H systems generating units. After deregulation, to describe bilateral contract for three area AGC, DISCO participation matrix is used. The performance of the system is studied for different operating cases. Simulation results revealed that the proposed controller damped out the frequency of oscillations and restore the system frequency and tie line power to set the value after the step load disturbance.*

***Keywords:*** *Automatic Generation Control, Bacterial Foraging, Capacitance Energy Storage, Deregulation, Sensitivity Analysis, Superconducting Magnetic Energy Storage.*

## 1. Introduction

The frequency of a power system is a very important performance signal to the system operator for stability and security considerations. The desired power system frequency should stay within a very small, acceptable interval around its nominal value. Otherwise, the operator needs to take relevant actions immediately. In the past decades, there are many research works on power system frequency regulation [1]–[4]. The early aim of the automatic generation control (AGC) is to regulate the power output of the electrical generator within a prescribed area in response to changes in system frequency, tie-line loading, so as to maintain the scheduled system frequency and interchange with the other areas with predetermined limits [1, 4]. As mentioned by Kundur [4], this function is commonly referred to as load-frequency control (LFC).

The problem of automatic frequency and tie-line flow regulation in power systems has a long history, from a control theoretic perspective. It is often viewed as one of the first and foremost large-scale, decentralised, robust controllers in engineering practice. The speed of the response is only limited by the natural time lags of the turbine, governor and the system itself. The supplementary speed control takes over the fine adjustment of the frequency by resetting the frequency error to zero through an integral action, the proportional-plus-integral (PI) controller [2]. The main drawback of this supplementary controller is that the dynamic performance of the system is highly dependent on the selection of its gain. A high gain may deteriorate the system performance having large oscillations and in most cases it causes instability [2–4]. Thus, the integrator gain must be set to a level that provides a compromise between a desirable transient recovery and low overshoot in the dynamic response of the overall system preventing instability [5, 6]. A lot of approaches have been reported in the literature to tune the gain of the PI controllers [1].

In general, the design of a controller for LFC can be divided into two groups. In first one, a tuning algorithm is used to tune the PID gains. Khodabakhshianand Hooshmand [7] used a symmetric tuning algorithm to tune a PID. The method strategy is based on maximum peak resonance specification and the main idea is to keep the maximum overshoot of the system response in a predetermined value following a step change in the reference input. In [8], the problem of AGC is considered as an optimisation problem. Thus, to carry out the optimisation actions, in a two-area power system, a gain scheduling PI control strategy is utilised for each area in which its gain will be obtained by using craziness- based particle swarm optimization algorithm. Similarly, Ali and Abd-Elazim [9] utilised the bacteria foraging optimisation algorithm to tune the PI gain in each area. Al-Hamouz et al. [10] suggested a design of

a sliding mode controller with chattering reduction feature applied to interconnected automatic generation control. After formulating the design of sliding mode controller as an optimisation problem, they utilised the genetic algorithm (GA) to find the optimal feedback gains and switching vector values of the controller. In the second group, researchers have attended to the self tuning techniques, types of the neural-networks and the fuzzy logic. In [11], a self-tuning PID fuzzy is used for the AGC. Oysal et al. [12] solved the LFC problem using dynamic wavelet neural network. In [13], Hemeida used a wavelet neural network to damp the frequency oscillations because of load changes. The energy storage resource may come from stationary units based on different technologies [14] (e.g. lead-acid, vanadium redox flow, fly wheels etc.) and from electric vehicles connected to the MG following the vehicle to grid concept [15, 16]. Different technologies such as flywheel [17], Battery Energy Storage (BES), Superconducting Magnetic Energy Storage (SMES), etc., can be adopted to alleviate system frequency fluctuation in isolated systems. Finally, robust controller of SMES for frequency control in the hybrid wind-diesel power system has been presented in [18].

In [19] the power systems with three areas are considered, the simulation is implemented by using MATLAB/Simulink Program and MATLAB Fuzzy Logic Toolbox (FLT), to damp out the oscillations, due to instantaneous load perturbations as fast as possible. In [20] has detailed model for the simulation of the SMES system and this model is intended to provide guidelines for a detailed SMES device simulation in the power system as well as to provide a basis for comparison of various simulation tools, control strategies, algorithms and realization approaches. References [21-22] made comprehensive mathematical model for the AGC of a two area interconnected hydrothermal power system fitted with SMES unit in either thermal or hydro area with generator rate constraints has been presented. It has been shown that these oscillations can be effectively damped out with the use of a small capacity SMES unit in either of the areas following a step load disturbance. Similarly like SMES, CES is one of the alternate energy storage for control the frequency oscillations in power system, [23-26] proposes new incorporation of storage devices in an interconnected power system for improved load frequency control.

## 2. Notation

| | |
|---|---|
| $f$ | Frequency |
| $K_{p=1,2,3}$ | Generator Gain Constant for area 1, 2 and 3 |
| $T_{p=1,2,3}$ | Generator Time Constant for area 1, 2 and 3 |
| $P_t$ | Turbine Output Power |
| $T_t$ | Turbine Time Constant |
| $P_g$ | Governor Output Power |
| $T_g$ | Governor Time Constant |
| $T_{ij}$ | Tie Line Coefficient |
| $K_{i=1,2,3}$ | Integral Controller Gains |
| $a_{ij}$ | Operator |
| $B_i$ | Bias Factor |
| $P_{ref}$ | The Output of ACE |
| $P_l$ | Electric Load Variations |
| $R$ | Speed Regulation Parameter |
| $T_w$ | Water Starting Time |
| $T$ | Time Constant of Hydro Governor |
| $K_p$ | Proportional gain of Hydro Governor |
| $K_d$ | Derivative gain of Hydro Governor |
| $K_i$ | Integral gain of Hydro Governor |
| $apf_i$ | Area Participation Factors |
| $cpf_i$ | Contract Participation Factors |
| $P_{i-jactual}$ | Tie Line Real Power |
| $p$ | Number of parameters to be optimized |
| $S$ | Number of bacteria |
| $N_s$ | Swimming length after tumbling of bacteria under in a chemotactic loop |
| $N_c$ | Number of iterations to be undertaken in a chemotactic loop |
| $N_{re}$ | Maximum number of reproduction to be undertaken |
| $N_{ed}$ | Maximum number of elimination and dispersal events |
| $P_{ed}$ | Probability with which elimination and dispersal will continue |
| H-T-H | Hydro-Thermal-Hydro |

## 3. Transfer Function Model of Supercoducting Magnetic Energy Storage (SMES)

Figure 1 shows the transfer function model SMES unit contained DC Superconducting coil and converter which are connected by Star-Delta/Delta-Star transformer. The control of the converter firing angle provides the DC voltage $E_d$ appearing across the inductor to be continuously varying within a certain range of positive and negative values. The inductor is initially charged to it's rated value $I_{do}$ by applying a small positive voltage. Once the current reaches the rated value, it is maintained constant by reducing the voltage across the inductor to zero since the coil is superconducting. Charge and discharge of SMES unit are controlled through change of commutation angle. In this study, as in recent literature [24-26] inductor voltage deviation of SMES unit of each area is based on

error of the same area in power system. Moreover the inductor current deviation is used as a negative feedback signal in SMES control Loop. So the current variable of SMES unit is intended to be settling its steady state value. If the load demand changes suddenly, the feedback provides the prompt restoration of current. The inductor current must be restored to its nominal value quickly after system disturbances, so that it can respond to the next load disturbance immediately. As a result, the equations of inductor voltage deviation and current deviation for each area in Laplace domain are as follows:

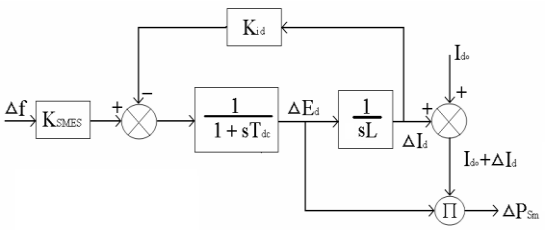


**Fig. 1** Tranfer Function Model of SMES

$$\Delta E(s) = K\frac{1}{1+ST}\Delta f(s) - K\frac{1}{1+ST}\Delta I(s) \quad (1)$$

$$\Delta I(s) = \frac{1}{SL}\Delta E(s) \quad (2)$$

Where, $K_{idi}$ is the gain for feedback. $\Delta I_{di}, T_{dci}$ is the change in increasing current, converter time delay, $K_{oi}$ (KV/Unit) is gain constant and $L_i$ (H) is the inductance of the coil. The deviation in the inductor real power of SMES unit is expressed in time domain $\Delta P_{smi}$ is.

$$\Delta P(t) = \Delta E\, I + \Delta I\, \Delta E \quad (3)$$

### 3.1 Frequency Deviation as a Control Signal

The frequency deviation Δf of the power system is sensed and used to control the SMES voltage, $E_d$. When power is to be pumped back in to the grid in the case of fall in the frequency due to sudden loading in the armature, the control voltage $E_d$ is to be negative since the current through the inductor and thyristor cannot change its direction. The incremental change in the voltage applied to the inductor is expressed as:

$$\Delta E_d = \left[\frac{K_f}{(1+ST_{dc})}\right][K_{Ai}(\Delta f_i + \frac{1}{B_i}\Delta P_{ij}) - K_{IAi}\Delta I_{di}] \quad (4)$$

$\Delta E_d$ is the incremental change in converter voltage, $T_{dc}$ is the converter time delay, $K_f$ is the gain of the control loop and S is the Laplace operator d/dt.

### 3.2 Area Control Error (ACE) As Control Signal

In case where tie line power deviation signals are available, it may be desirable to use ACE as input to SMES control logic. This has certain disadvantages, as compared to frequency deviation derived controls. The area control error of two areas is defined as:

$$ACE_i = \Delta P_{ij} + B_i \Delta f_i \quad (5)$$

Where, i,j=1,2, $\Delta f_i$ = Change in frequency of area, i. $\Delta P_{ij}$ = Change in tie line power flow out of area i to j. If ACE is directly used for the control of SMES, The gains constant $K_A$ (KV/unit Area) would be totally different from $K_f$, the gain constant for frequency deviation as control signal. So a signal proportional to area control error ($\Delta f_i$ + $(1/B_i)\Delta P_{ij}$) is used in such a scheme. Then,

$$\Delta E_{di} = \frac{K_{Ai}}{(1+ST_{dci})}(\Delta f_i + \frac{1}{B_i}\Delta P_{ij}) \quad (6)$$

### 4.0 Transfer function model of Capacitive Energy Storage (CES)

Capacitor is an electrochemical device consisting of two porous electrodes, an ion exchange membrane separating the two electrodes and a potassium hydroxide electrolyte. In many ways, an capacitor is subject of same physics as a standard capacitor. That is the capacitor is determined by [23-24] the effective area of the plates, the separation distances of the electrode and the dielectric constant of the separating medium. The operation of CES units, that is, charging, discharging, the steady state model and the power modulation during dynamic oscillatory period, is controlled by the application of the proper voltage to the capacitor so that the desired current flows in to or out of the CES. This can be achieved by controlling the firing angle of the converter bridges. Fig 2 shows the transfer function model CES in this, incremental change in CES current is expressed as.

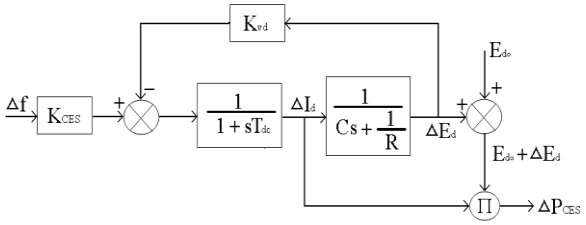


**Fig. 2.** Tranfer Function Model of CES

$$\Delta I_{di} = \left[\frac{K_{cfi}}{(1+ST_{dci})}\right]\Delta f \quad (7)$$

Where, i= 1,2…, $\Delta I_{di}$ is the incremental change in current of CES unit(KA),$T_{dci}$ is the converter time delay(sec),$K_{cfi}$ is the gain of the control loop(KA/Hz), s is the Laplace operator(d/dt) and i denotes the area. The gains constant $K_{ci}$ (KA/unit Area) would be totally different from $K_{cf}$, the gain constants for frequency as control signal. So a signal proportional to area control error ($\Delta f_i$ + $(1/B_i)$ $\Delta P_{ij}$) is used in such a scheme. Then,

$$\Delta I_{} = \frac{K_{}}{(1+ST_{})}(\Delta f + \frac{1}{B}\Delta P) \qquad (8)$$

where i,j=1,2,3.

The capacitor voltage deviation can be sensed and used as a negative feed back signal in the CES control loop to achieve quick restoration of voltage then, that with frequency deviation as control signal,

$$\Delta I_{di} = \frac{1}{(1+ST_{dci})}(K_{cfi}\Delta f_i - k_{vdi}\Delta E_{di}) \qquad (9)$$

Where $K_{vdi}$ (KA/KV) is the gain corresponding to the $\Delta E_d$ feedback.

**5.0 Discrete Model of Three Area H-T-H system after Deregulation:**

A discrete signal or discrete-time signal is a time series, perhaps a signal that has been sampled from a continuous-time signal. Unlike a continuous-time signal, a discrete-time signal is not a function of a continuous-time argument, but is a sequence of quantities; that is, a function over a domain of discrete integers. Each value in the sequence is called a sample. When a discrete-time signal is a sequence corresponding to uniformly spaced times, it has an associated sampling rate; the sampling rate is not apparent in the data sequence, so may be associated as a separate data item. In mathematics, discretization concerns the process of transferring continuous models and equations into discrete counterparts. This process is usually carried out as a first step toward making them suitable for numerical evaluation and implementation on digital computers. The continuous-time dynamic system is modeled by the linear vector differential equations:

$$\dot{X} = AX + BU + \Gamma p \qquad (10)$$

The discrete-time behavior of the continuous-time system is modeled by the system of first-order linear difference equations and these equations are listed in Appendix I.

$$X(k+1) = \Phi X(k) + \Psi U(k) + Yp(k) \qquad (11)$$

X(k), U(k) and p(k) have the same dimensions as in the continuous-time description and are specified at t= kT, k=0,1,.. etc. T is the sampling period. Unless otherwise stated X(k) indicates X(kT). That is, X(k) implies the vector X(t) at t = kT. k is the sampling instant. Φ, Ψ, Y are the state transition, control transition and disturbance transition matrices. These matrices depend on the sampling period T. Once T is fixed, these matrices become time invariant. The introduction of the discretization requires that the inputs be piece wise constant functions of time and the, changes in the value of U and p occur only at the sampling instants. The matrices are evaluated using the following relations,

$$\begin{aligned} \Phi &= e^{AT} \\ \Psi &= (e^{AT} - I)B \\ Y &= (e^{AT} - I)A^{-1}\Gamma \end{aligned} \qquad (12)$$

Where I is an identity matrix. Exact discretization may sometimes be intractable due to the heavy matrix exponential and integral operations involved. It is much easier to calculate an approximate discrete model, based on that for small time steps $e^{AT} \approx I + AT$ The approximate solution then becomes, corresponding three area H-T-H system state equations are given on Appendix-1:

$$\Phi = I + AT$$
$$\Psi = BT$$
$$Y = \Gamma T$$

Therefore :

$$X(k+1) = (I + AT)X(k) + (BT)U(k) + (\Gamma T)p(k)$$

**6.0 DISCO Participation Matrix**

In restructured environment, Discos has liberty to purchase power from any GENCOs at competitive prices. They may or may not be in their own area. The concept of Disco Participation Matrix (DPM) is introduced in the restructured environment. In DPM matrix the number of rows equal to the number of GENCOs present in the system and number of column is equal to the number of Discos. In this, three area system is considered in which each area has three GENCOs and three DISCOs as shown in Fig. 3. The corresponding DPM will become. Here Cpf is the contract participation factor. In DPM diagonal element shows the local demand and off diagonal element shows the demand of the Discos in one area to the Gencos in another area. The sum of all the entries in a column in this matrix is unity. In this paper value of DPM is

$$\text{DPM} = \begin{bmatrix} 0.2 & 0.15 & 0.3 & 0.4 & 0.2 & 0 \\ 0.3 & 0.15 & 0.1 & 0.2 & 0.15 & 0.2 \\ 0.3 & 0.15 & 0.1 & 0 & 0.15 & 0 \\ 0.1 & 0.15 & 0.4 & 0.2 & 0.2 & 0.2 \\ 0 & 0.2 & 0.1 & 0 & 0.15 & 0 \\ 0.1 & 0.2 & 0 & 0.2 & 0.15 & 0.6 \end{bmatrix}$$

$$Genco_{1scheduled} = (0.2+0.15+0.3+0.4+0.2+0)0.01 = 0.0125$$
$$Genco_{2scheduled} = (0.3+0.15+0.1+0.2+0.15+0.2)0.01 = 0.011$$
$$Genco_{3scheduled} = (0.3+0.15+0.1+0+0.15+0)0.01 = 0.007$$

$$Genco_{4scheduled} = (0.1+0.15+0.4+0.2+0.2+0.2)0.01 = 0.0125$$
$$Genco_{5scheduled} = (0+0.2+0.1+0+0.15+0)0.01 = 0.008$$
$$Genco_{6scheduled} = (0.1+0.2+0+0.2+0.15+0.6)0.01 = 0.0125$$

The block diagram for three-area H-T-H AGC system is formulated in the deregulated environment. The coefficient which represent their sharing, are called as "ACE participation factor (apf)". The sum of apf of each area equals to unity and $\Sigma apf_i = 1$ where n is the number of GENCOs in each area. In the case of three-area power system, scheduled steady state power flow on any tie-line is given as follows:

$\Delta P_{i\text{-}j\ scheduled}$ = [Demands of DISCOs in area j from GENCOs in area i] - [Demand of DISCOs in area i from GENCOs in area j] (14)

and

$$\Delta P_{1\text{scheduled}}(k) = \Delta P_{1-2scheduled}(k) + a_{31}\,\Delta P_{3-1scheduled}(k) \quad (15)$$
$$\Delta P_{2\text{scheduled}}(k) = \Delta P_{2-3scheduled}(k) + a_{12}\,\Delta P_{1-2scheduled}(k) \quad (16)$$
$$\Delta P_{3\text{scheduled}}(k) = \Delta P_{3-1scheduled}(k) + a_{23}\,\Delta P_{2-3scheduled}(k) \quad (17)$$

where $a_{12}= a_{23}= a_{31}$ are different and not equal to -1, because in this study it is taken as $P_{r1} = P_{r2}= P_{r3}$ such that $P_{r1,}$ $P_{r2}$ and $P_{r3}$ are rated power of areas and k is sampling index. The error for the power defined in (1)-(3) is given as follows:

$$\Delta P_{\text{ierror}} = \Delta P_{iactual} + \Delta P_{ischeduled}$$

The error signal is used to generate its ACE signals in the steady state as follows:

$$ACE_i = B_i \Delta f_{ierror} + \Delta P_{ierror}; where\ i = 1,2,3 \quad (19)$$

In the case of bilateral contracts, new configuration of AGC at power system as block diagram is given in Fig. 3.

**7.0 Bacterial Foraging**

Bacterial Foraging is an optimization technique. This technique is based on the foraging behavior of e.coli. bacteria. The e.coli. bacteria present in the human intestine. This technique is subdivided into four steps chemotaxis, swarming, reproduction, elimination and dispersal as refered in [9].

**a) Bacterial Foraging Algorithm**

In case of BF technique we assign each bacterium with a set of variables to be optimized and are assigned with random values (Δ)within the universe of discourse defined through upper and lower limit between which the optimum value is likely to fall. Each bacterium is allowed to take all possible values within the range and the objective function which is ISE defined by following is minimized.

$$ISE = \Delta f_1^2 + \Delta f_2^2 + \Delta f_3^2 + \Delta P_{tie12} + \Delta P_{tie23} + \Delta P_{tie31} \quad (20)$$

Step 1 Initialization

1. Number of parameters (p) to be optimized;
2. Number of bacteria (S) to be used for searching the total region;
3. Swimming length ($N_s$) after which tumbling of bacteria will be undertaken in a chemotactic loop;
4. $N_c$ the number of iterations to be undertaken in a chemotactic loop ($N_c > N_s$)
5. $N_{re}$ the maximum number of reproduction to be undertaken;
6. $N_{ed}$ the maximum number of elimination and dispersal events to be imposed over the bacteria;
7. $P_{ed}$ the probability with which the elimination and dispersal will continue;
8. The location of each bacterium P(1-p,1-S,1) which is specified by random numbers within [ 1,1];
9. The value of C(i) which is assumed to be constant in our case for all of the bacteria to simplify the design strategy
10. The values of $d_{attract}$, $W_{attract}$, $h_{repelent}$ and $W_{repelent.}$ In this simulation work, we have considered: S=10, $N_c$=50, $N_s$=4, $N_{re}$=15, $N_{ed}$=2, $P_{ed}$=0.25, $d_{attract}$=0.1, $W_{attract}$=0.2, $h_{repelent}$=0.1, $W_{repelent}$=10.

Step 2 Iterative Algorithm for Optimization

This section models the bacterial population chemotaxis, swarming, reproduction, elimination, and dispersal (initially, j = k = l = 0). For the algorithm, updating $\theta^i$ automatic results in updating "P".

Step i) Elimination-dispersal loop $l = l+1$.

Step ii) Reproduction loop $k = k+1$.

Step iii) Chemotaxis loop $j = j+1$.

*For i=1,2..S, calculate the cost function value for each bacterium as follows:*

- *Compute the value of cost function* $J(i, j, k, l)$.
  Let $J_{sw}(i, j, k, l) = J(i, j, k, l) + J_{cc}(\theta^i(j, k, l), P(j, k, l))$ (i.e., add on the cell-to-cell attractant effect for swarming behavior).
- Let $J_{last} = J_{sw}(i, j, k, l)$ to save this value since we may find a better cost via a run.

End of for loop.

*For i=1,2..S, take the tumbling/swimming decision*

- Tumble: Generate a random vector $\Delta(i) \in \Re^p$ with each element $\Delta_m(i)$ $m = 1, 2, ..., p$, a random number on [ 1,1].
- Move: let $\theta^i(j+1,k,l) = \theta^i(j,k,l) + C(i)\frac{\Delta(i)}{\sqrt{\Delta^T(i)\Delta(i)}}$, The fixed step size in the direction of tumble for bacterium is considered.
- Compute $J(i, j+1, k, l)$ and then $J_{sw}(i, j+1, k, l) = J(i, j+1, k, l) + J_{cc}(\theta^i(j+1, k, l), P(j+1, k, l))$ .
- Swim:
  i) let $m = 0$ ; (counter for swim length);
  ii) while $m < N_s$ (have not climbed down too long).
  - Let m=m+1
  - if $J_{sw}(i, j+1, k, l) < J_{last}$ (if doing better), let $J_{last} = J_{sw}(i, j+1, k, l)$ and let $\theta^i(j+1, k, l) = \theta^i(j, k, l) + C(i)\frac{\Delta(i)}{\sqrt{\Delta^T(i)\Delta(i)}}$ and use this $\theta^i(j+1, k, l)$ to compute the new $J(i, j+1, k, l)$ .
  - Else, let $m = N_s$ . This is the end of the while statement.

*Go to the next bacterium* $(i+1)$ *if* $i \neq S$ *(i.e., go to ii) to process the next bacterium.*

Step iv) If $j < N_c$ , go to Step iii). In this case, continue chemotaxis since the life of the bacteria is not over.

Step v) Reproduction

a) For the given $k$ and $l$ , and for each i=1,2,…S,let $J^i_{health} = \min_{j \in \{1...N_c\}}\{J_{sw}(i, j, k, l)\}$ be the health of the bacterium $i$ . Sort bacteria in order of ascending cost $J_{health}$ .

b) The $S_r$=S/2 bacteria with the highest $J_{health}$ values die and other $S_r$ bacteria with the best value split.

Step vi) If $k < N_{re}$ , go to (ii) In this case, we have not reached the number of specified reproduction steps, so we start the next generation in the chemotactic loop.

Step vii) Elimination dispersal: For $i = 1, 2, ..., S$ , with probability $P_{ed}$ , eliminate and disperse each bacterium to a random location on the optimization domain.

**8.0 Result Discussion**

The proposed BF based approach for solving the LFC was applied to three area H-T-H system with different cases. The program was written in MATLAB and executed on a PC with Intel(R) core (TM) i3 CPU with 2.13 GHz processor. The Simulations results are presented. For the optimum AGC controller gain value, the corresponding results of optimum generators participations in generations, tie line exchanges obtained by computed values using formulae and MATLAB-Simulink based results for case study where are computed.

Comparative performance of three Area H-T-H AGC under deregulated environment with open loop, with conventional controller, with BF controller. During the simulation study, error signals $\Delta f_1$, $\Delta f_2$, $\Delta f_3$ and $\Delta P_{tie}$ are required for the controller is transferred to BF algorithm. All positions of bacterial particles on each dimension area clamped in limits which are specified by the user, a step increase in demand of 0.01p.u is applied in any one of the area. Simulation result shows that the performance improvement in time domain specifications for a step load of 0.01p.u. Using the BF approach, global and local solutions could be simultaneously found for better tuning of the controller parameters. The integral value which was obtained by the BF algorithm is compared with that of the one derived from Trial and Error method in various perspectives, namely robustness and stability, performance.

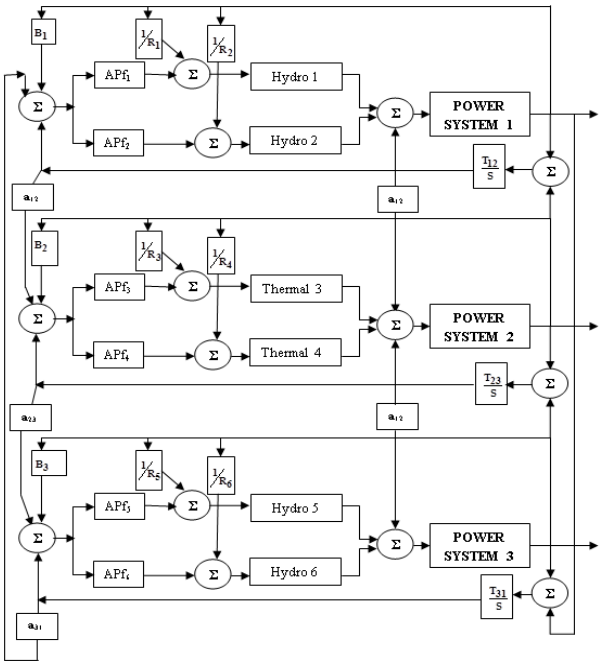


**Fig. 3** MATLAB-SIMULINK Transfer function model of Three area H-T-H under deregulated environment using SMES and CES

In figure 3 shows the transfer function model of three areas H-T-H with 1% disturbance is given in all the three areas (Uncontrolled mode). Fig. 4 show the dynamic responses of frequency deviations in three areas (i.e.,$\Delta f_1$, $\Delta f_2$ and $\Delta f_3$) and the tie line power deviation ($\Delta P_{tie1\text{-}2,}$ ($\Delta P_{tie2\text{-}3}$ and ($\Delta P_{tie3\text{-}1}$) for the three area Hydro-Thermal-Hydro power system. Comparison made between without controller, with controller and with BF based integral controller. These graph concluded that BF based integral controller give less settling time and low peak overshoot. Figure 5 shows the bar graph in which the diagonal lines graph shows the graph of with controller and dotted graph shows the graph of with BF based integral controller and these values are tabulated and compared in Table.1. Fig. 6 shows the response of three area H-T-H system with 1% disturbance is given to the first area (Controlled mode) with the dynamic responses of frequency deviations in three areas (i.e.,$\Delta f_1$, $\Delta f_2$ and $\Delta f_3$) and` the tie line power deviation ($\Delta P_{tie1\text{-}2,}$ ($\Delta P_{tie2\text{-}3}$ and ($\Delta P_{tie3\text{-}1}$) for the three area Hydro-Thermal-Hydro power system. It is evident that, the BF based integral controller has given the performance quite superior in terms of settling time and peak overshoot to that of integral controller and the obtained values are compared in Table 2 as well in tems of bar graph as shown in fig.7.

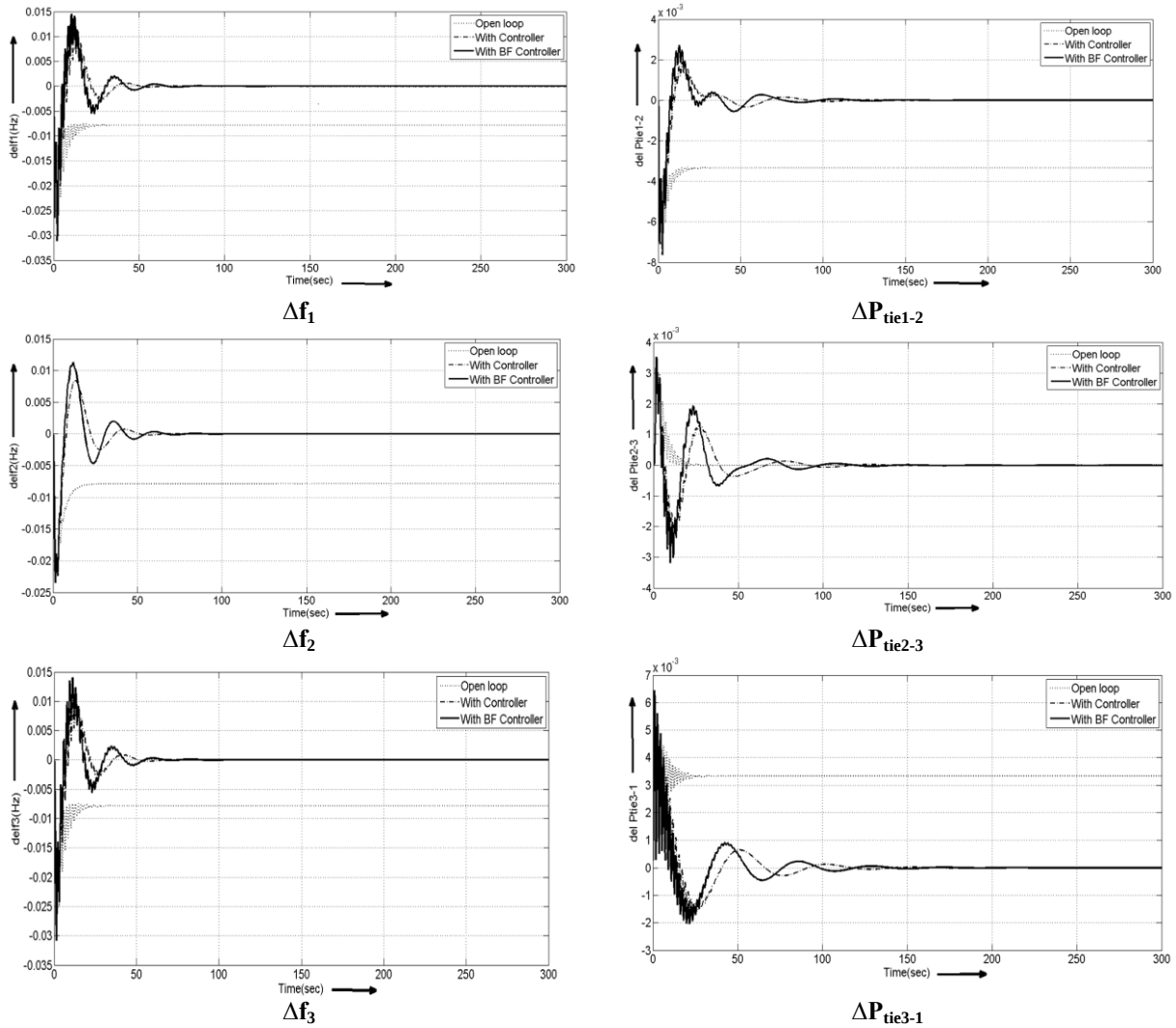


$\Delta f_1$ $\Delta P_{tie1\text{-}2}$

$\Delta f_2$ $\Delta P_{tie2\text{-}3}$

$\Delta f_3$ $\Delta P_{tie3\text{-}1}$

**Fig. 4** MATLAB-SIMULINK Transfer function model of Three area H-T-H under deregulated if 1% load is applied in all the three areas

In figure 3 shows the transfer function model of three areas H-T-H with 1% disturbance is given in all the three areas (Uncontrolled mode). Fig. 4 show the dynamic responses of frequency deviations in three areas (i.e.,$\Delta f_1$, $\Delta f_2$ and $\Delta f_3$) and the tie line power deviation ($\Delta P_{tie1\text{-}2,}$ ($\Delta P_{tie2\text{-}3}$ and ($\Delta P_{tie3\text{-}1}$) for the three area Hydro-Thermal-Hydro power system. Comparison made between without controller, with controller and with BF based integral controller. These graph concluded that BF based integral controller give less settling time and low peak overshoot. Figure 5 shows the bar graph in which the diagonal lines graph shows the graph of with controller and dotted graph shows the graph of with BF based integral controller and these values are tabulated and compared in Table.1. Fig. 6 shows the response of three area H-T-H system with 1% disturbance is given to the first area (Controlled mode) with the dynamic responses of frequency deviations in three areas (i.e.,$\Delta f_1$, $\Delta f_2$ and $\Delta f_3$) and` the tie line power deviation ($\Delta P_{tie1\text{-}2,}$ ($\Delta P_{tie2\text{-}3}$ and ($\Delta P_{tie3\text{-}1}$) for the three area Hydro-Thermal-Hydro power system. It is evident that, the BF based integral controller has given the performance quite superior in terms of settling time and peak overshoot to that of integral controller and the obtained values are compared in Table 2 as well in tems of bar graph as shown in fig.7.

**Table 2:** Settling Time and Maximum Peak Overshoot of three-area Hydro-Thermal-Hydro system

| | **Settling Time** | | | **Peak Overshoot** | | |
|---|---|---|---|---|---|---|
| | $\Delta f_1$ | $\Delta f_2$ | $\Delta f_3$ | $\Delta f_1$ | $\Delta f_2$ | $\Delta f_3$ |
| **With Controller** | **73 s** | **80 s** | **75 s** | **0.021s** | **0.016s** | **0.021s** |
| **With BF Controller** | **70 s** | **75 s** | **70 s** | **0.022s** | **0.016s** | **0.021s** |

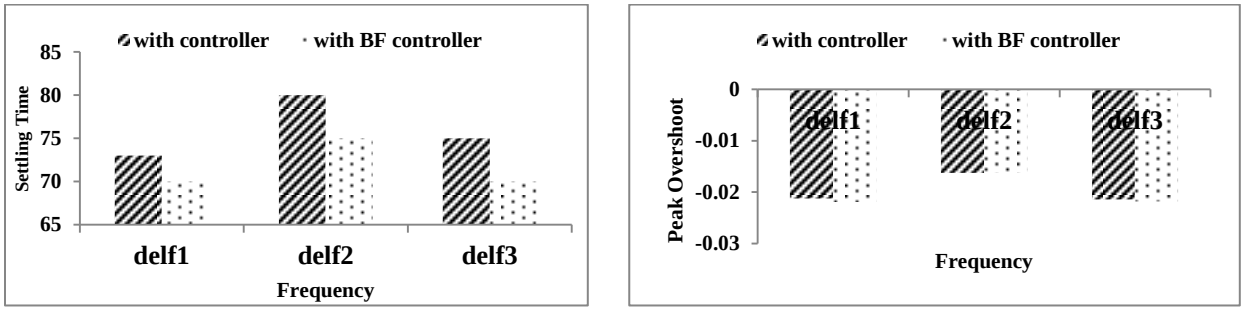


**(a)** **(b)**

**Fig. 5:** (a) Settling time (b) Peak overshoot of three area Hydro-Thermal-Hydro system

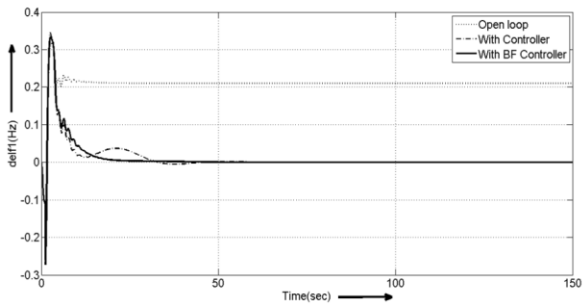


$\Delta f_1$

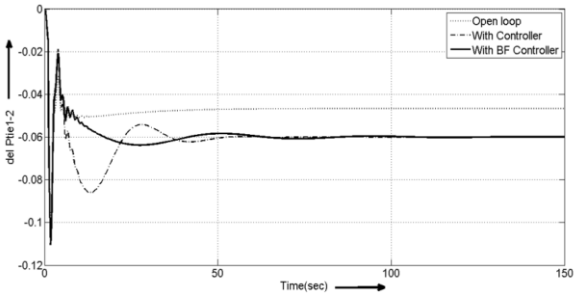


$\Delta P_{tie1\text{-}2}$

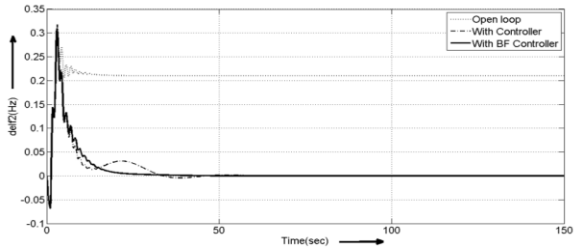


$\Delta f_2$

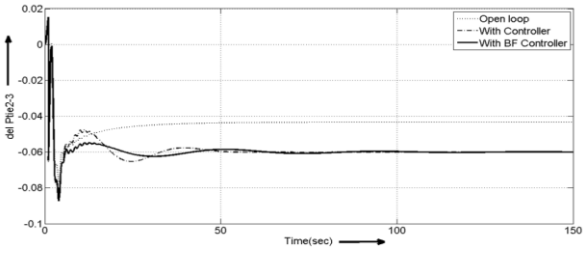


$\Delta P_{tie2\text{-}3}$

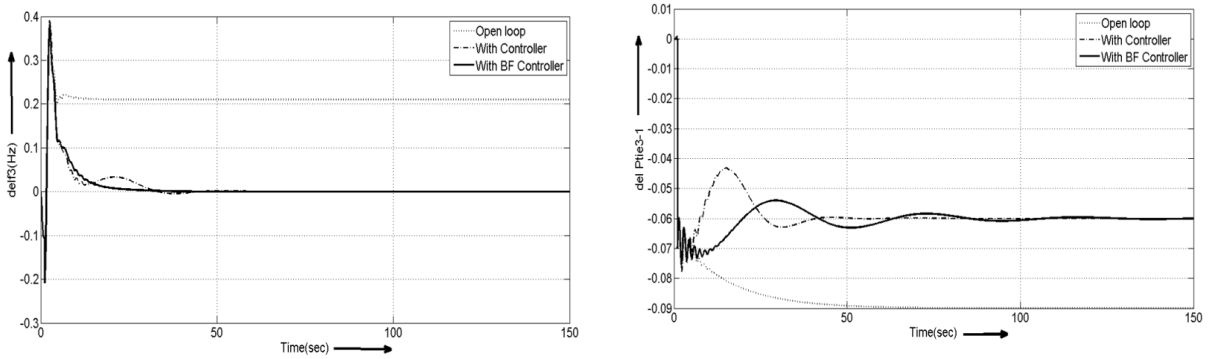


$\Delta f_3$ $\Delta P_{tie3-1}$

**Fig. 6** MATLAB-SIMULINK Transfer function model of Three area H-T-H under deregulated environment if 1% load is applied to first area

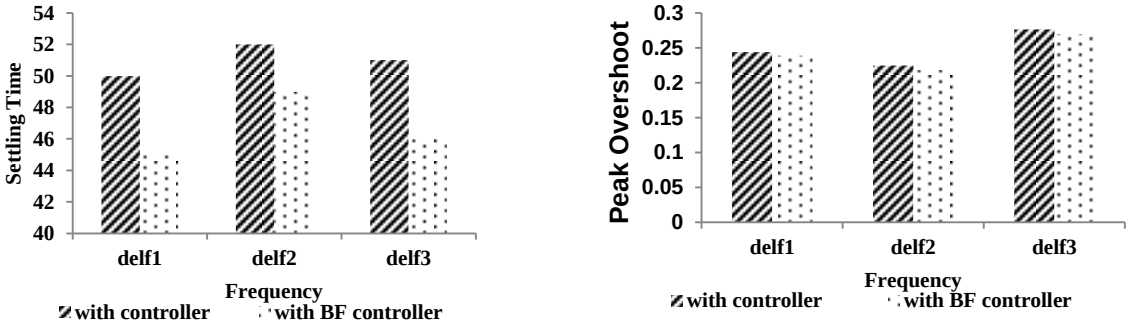


**(a)** **(b)**

**Fig. 7:** (a) Settling time (b) Peak overshoot of three area Hydro-Thermal-Hydro system

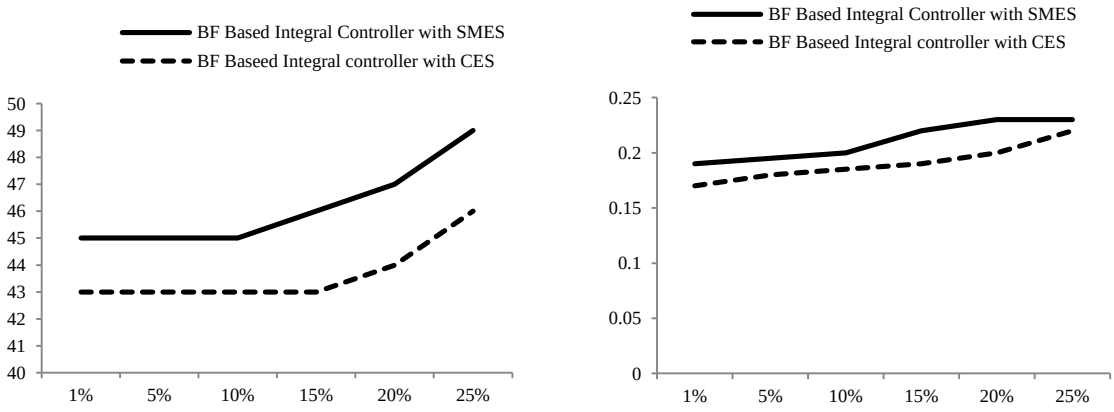


(a) Settling Time (b) Peak Over Shoot

**Fig. 8** Settling Time & Peak Over Shoot between proposed BF controller based SMES and CES Energy Storage Devcices under various Load Conditions

**Table-2** Settling Time and Maximum Peak Overshoot of two-area Hydro-Thermal-Hydro system in deregulated environment

| | Settling Time | | | Peak Overshoot | | |
|---|---|---|---|---|---|---|
| | **delf1** | **delf2** | **delf3** | **delf1** | **delf2** | **delf3** |
| **With Controller** | 50 s | 52 s | 51 s | 0.24399s | 0.2246s | 0.2765 s |
| **With BF Controller** | 45 s | 49 s | 46 s | 0.2389 s | 0.2183s | 0.2697 s |

Comparative analysis: From the fig.8 shows bar chart shows the settling time, peakover shoot performance of proposed SMES and CES are close to each other in the context of transient analysis particularly under deregulated environment. But CES is practically maintenance free, it does not impose any environmental problem, and it is quite simple and less expensive. CES damping effects are slightly better than SMES when variation in load.

## CONCLUSION

Modified AGC after deregulation, is an important issue in power system. AGC of a three area power system having power generation from H-T-H has been studied and ACE parameters are optimized for an appropriate performance index by using BF. Further to improve the system performance, particularly with the presence of uncertainties, this paper focuses the effect of SMES and CES frequency controllers are successfully implemented in three area power system. Finally comparative studies have been made between two energy storage devices. By this method a simple controllers is designed, and it is found that this work may seems to be quite simple and easy to analyze in real power system. It has given very good results in terms of performance and stability. The Simulation result clearly shows that proposed method is robust to change in system parameters and it has given better performance than conventional integral controller. Performance of proposed frequency controllers, SMES and CES are close to each other in the context of transient analysis. But CES is practically maintenance free, it does not impose any environmental problem, and it is quite simple and less expensive. CES damping effects slightly better than SMES when variation in load for LFC problem in deregulated environment

References:


[1] P. M. Anderson and M. Mirheydar, "A low-order system frequency response model," IEEE Trans. Power Syst.,vol.5,no.3,pp.720–729, Aug. 1990.

[2] P. M. Anderson and M. Mirheydar, "An adaptive method for setting under frequency load shedding relays," IEEE Trans. Power Syst., vol. 7, no. 2, pp. 647–655, May 1992.

[3] H.Saadat, Power System Analysis,2nded. New York: McGraw-Hill, 2002.

[4] P. Kundur, Power System Stability and Control. Palo Alto, CA: EPRI, 1994.

[5] Tripathy, S.C., Chandramohanan, P.S., Balasubramanium, R.: 'Self tuning regulator for adaptive load frequency control of power system', J. Inst. Eng. (India), 1998,79, (2), pp. 103–108.

[6] Xu, X., Mathur, R.M., Jiang, J., Rogers, G.J., Kundur, P.: 'Modeling of generators and their controls in power system simulations using singular perturbations', IEEE Trans. Power Syst., 1998, 13, (1), pp. 109–114.

[7] Khodabakhshian, A., Hooshmand, R.: 'A new PID controller design for automatic generation control of hydro power systems', Electr. Power Energy Syst., 2010,32, (5), pp. 375–382.

[8] Gozde, H., Taplamacioglu, M.C.: 'Automatic generation control application with craziness based particle swarm optimization in a thermal power system', Electr. Power Energy Syst., 2011,33, (1), pp. 8–16.

[9] Ali, E.S., Abd-Elazim, S.M.: 'Bacteria foraging optimization algorithm based load frequency controller for interconnected power system', Electr. Power Energy Syst., 2011,33, pp. 633–638.

[10] Al-Hamouz, Z., Al-Duwaish, H., Al-Musabi, N.: 'Optimal design of a sliding mode AGC controller: application to a nonlinear interconnected model', Electr. Power Syst. Res., 2011,81, (7), pp. 1403–1409.

[11] Yesil, E., Guzelkaya, M., Eksin, I.: 'Self tuning fuzzy PID type load and frequency controller', Energy Convers. Manag., 2004,45, (3), pp. 377–390.

[12] Oysal, Y., Yilmaz, A.S., Koklukaya, E.: 'A dynamic wavelet network based adaptive load frequency control in power systems', *Electr.Power Energy Syst.*, 2005, 27, (1), pp. 21–29.

[13] Hemeida, A.M.: 'Wavelet neural network load frequency controller', *Energy Convers. Manag.*, 2005, 46, (9–10), pp. 1613–1630.

[14] Divya, K.C., stergaard, J.: 'Battery energy storage technology for power systems– an overview', Electr. Power Syst. Res., 2009, 79, (4), pp. 511–520.

[15] Lopes,J.A.P.,Soares,F.J.,Almeida,P.M.R.:'Integrationof electricvehicles in the electric power system', Proc. IEEE, 2011,99, (1), pp. 168–183.

[16] Vazquez, S., Lukic, S.M., Galvan, E., Franquelo, L.G., Carrasco, J.M.: 'Energy storage systems for transport and grid applications', IEEE Trans. Ind. Electron., 2010,57, (12), pp. 3881–3895.

[17] Takahashi, R, and Tamura, J. Frequency stabilization of small power system with wind farm by using flywheel energy storage system. *Proc. of IEEE Int symp of Diagnostics for Electric Machines, Power electronics and Drives* 2007; pp.393-398.

[18] Issarachai Ngamroo. Robust Frequency Control of Wind-Diesel Hybrid Power System Using Superconducting Magnetic Energy Storage. *Int Journal of Emerging Electric Power Systems*, Vol.10, Issue2, 2009 Article 3; pp 1-26.

[19] Demiroren, E. Yesil. Automatic generation control with fuzzy logic controllers in the power system including SMES units. *Electrical Power and Energy Systems* 26 (2004); pp. 291–305.

[20] IEEE Task Force on Benchmark Models for Digital Simulation of FACTS and Custom-Power Controllers, T&D Committee. Detailed Modeling of Superconducting Magnetic Energy Storage (SMES) System. *IEEE Transactions On Power Delivery*, Vol. 21, no.2, April 2006: pp 699-710.

[21] Rajesh Joseph Abraham, D. Das, Amit Patra. Automatic generation control of an interconnected hydrothermal power system considering superconducting magnetic energy storage. *Electrical Power and Energy Systems* 29 (2007); pp. 571–579.

[22] Akira Taguchi, Tadakazu Imayoshi, Takashi Nagafuchi, Takahiro Akine, Nobuhiro Yamada,and Hidemi Hayashi. A Study of SMES Control Logic for Power System Stabilization. *IEEE Transactions On Applied Superconductivity*, Vol.17, no.2, June 2007, pp 2343-2346.

[23] Mairaj ud din Mufti, Shameem Ahmad Lone, Shiekh Javed Iqbal, Muzzafar Ahmad, Mudasir Ismail. Super-capacitor based energy storage system for improved load frequency control. *Electric Power Systems Research* 79, 2009; pp 226–233.

[24] J. Raja, C. Christober Asir Rajan, *"Comparative Analysis and Effect of CES on AGC by Using ANN ",* Iranian Journal of Electrical and Computer Engineering (IJECE), Paper Number: 874.2010.04.22, Vol.10, No.01, Winter-Spring 2011, ISSN 1682-0053.

[25] J. Raja, Dr. C. Christober Asir Rajan, *" FUZZY Controlled SMES Unit for Damping Power System Oscillations in a Combined Cycle Gas Turbine ",* Journal of Electrical Engineering: Volume 11 / 2011 - Edition : 1, ISSN: 1582-4594, pp 36-45.

[26] J. Raja , Dr. C. Christober Asir Rajan , *" Improved Power System Dynamic Performance Using SMES For Frequency Excursion",* Journal Electrical Systems, ESR Group, Volume 7, Issue 2, (June 2011), ISSN 1112-5209, pp 193-205.

## Appendix A

The state space equations of the power system are given in Laplace domain as follows:

$$\Delta\omega_1(s)=\frac{K_{P1}}{1+sT_{P1}}(\Delta P_{t1}(s)+\Delta P_{t2}(s)-\Delta P_{l1}(s)-\Delta P_{l2}(s)-\Delta P_{tie1\text{-}2}(s)-a_{31}\Delta P_{tie3\text{-}1}(s)) \quad (A.1)$$

$$\Delta\omega_2(s)=\frac{K_{P2}}{1+sT_{P2}}(\Delta P_{t3}(s)+\Delta P_{t4}(s)-\Delta P_{l3}(s)-\Delta P_{l4}(s)-\Delta P_{tie2\text{-}3}(s)-a_{12}\Delta P_{tie1\text{-}2}(s)) \quad (A.2)$$

$$\Delta\omega_3(s)=\frac{K_{P3}}{1+sT_{P3}}(\Delta P_{t5}(s)+\Delta P_{t6}(s)-\Delta P_{l5}(s)-\Delta P_{l6}(s)-\Delta P_{tie3\text{-}1}(s)-a_{23}\Delta P_{tie2\text{-}3}(s)) \quad (A.3)$$

$$\Delta P_{t1}(s)=\frac{1}{1+sT_{t1}}\Delta P_{g1}(s) \quad (A.4)$$

$$\Delta P_{t2}(s)=\frac{1}{1+sT_{t2}}\Delta P_{g2}(s) \quad (A.5)$$

$$\Delta P_{t3}(s)=\frac{1-sT_w}{1+0.5sT_w}\Delta P_{r1}(s) \quad (A.6)$$

$$\Delta P_{t4}(s)=\frac{1-sT_w}{1+0.5sT_w}\Delta P_{r2}(s) \quad (A.7)$$

$$\Delta P_{t5}(s)=\frac{1}{1+sT_{t5}}\Delta P_{g5}(s) \quad (A.8)$$

$$\Delta P_{t6}(s)=\frac{1}{1+sT_{t6}}\Delta P_{g6}(s) \quad (A.9)$$

$$\Delta P_{r1}(s)=\frac{1+sT_r}{1+sT_2}\Delta P_{g3}(s) \quad (A.10)$$

$$\Delta P_{r2}(s)=\frac{1+sT_r}{1+sT_4}\Delta P_{g4}(s) \quad (A.11)$$

$$\Delta P_{g1}(s)=\frac{1}{1+sT_{g1}}(apf_1\Delta P_{ref1}(s)-\frac{1}{2\pi R_1}\Delta\omega_1(s)) \quad (A.12)$$

$$\Delta P_{g2}(s)=\frac{1}{1+sT_{g2}}(apf_2\Delta P_{ref1}(s)-\frac{1}{2\pi R_2}\Delta\omega_1(s)) \quad (A.13)$$

$$\Delta P_{g3}(s)=\frac{1}{1+sT_1}(apf_3\Delta P_{ref2}(s)-\frac{1}{2\pi R_3}\Delta\omega_2(s)) \quad (A.14)$$

$$\Delta P_{g4}(s)=\frac{1}{1+sT_3}(apf_4\Delta P_{ref2}(s)-\frac{1}{2\pi R_4}\Delta\omega_2(s)) \quad (A.15)$$

$$\Delta P_{g5}(s)=\frac{1}{1+sT_{g5}}(apf_5\Delta P_{ref3}(s)-\frac{1}{2\pi R_5}\Delta\omega_3(s)) \quad (A.16)$$

$$\Delta P_{g6}(s)=\frac{1}{1+sT_{g6}}(apf_6\Delta P_{ref3}(s)-\frac{1}{2\pi R_6}\Delta\omega_3(s)) \quad (A.17)$$

$$\Delta P_{ref1}(s)=\frac{-K_{i1}}{s}(\frac{B_1}{2\pi}\Delta\omega_1(s)+\Delta P_{12}(s)+a_{31}\Delta P_{31}(s)) \quad (A.18)$$

$$\Delta P_{ref2}(s)=\frac{-K_{i2}}{s}(\frac{B_2}{2\pi}\Delta\omega_2(s)+\Delta P_{23}(s)+a_{12}\Delta P_{12}(s)) \quad (A.19)$$

$$\Delta P_{ref3}(s)=\frac{-K_{i3}}{s}(\frac{B_3}{2\pi}\Delta\omega_3(s)+\Delta P_{31}(s)+a_{23}\Delta P_{23}(s)) \quad (A.20)$$

$$\Delta P_{12}(s)=\frac{T_{12}}{2\pi s}(\Delta\omega_1(s)-\Delta\omega_2(s)) \quad (A.21)$$

$$\Delta P_{23}(s)=\frac{T_{23}}{2\pi s}(\Delta\omega_2(s)-\Delta\omega_3(s)) \quad (A.22)$$

$$\Delta P_{31}(s)=\frac{T_{31}}{2\pi s}(\Delta\omega_3(s)-\Delta\omega_1(s)) \quad (A.23)$$

## Appendix B

*Thermal Data : $K_{pi}$=120Hz/P.u. Mw, $T_p$=20S, $a_{ij}$=-1,$T_{ij}$=0.086s, $T_t$=0.3s, $T_g$=0.08s, R=2.4Hz/p.u.Mw*
*Hydro Data : $K_p$=1.7, $K_d$=1.4, $K_i$=1.9, $T_p$=20s, $T_W$=1s, f=50Hz*